Identifying defects in multiferroic nanocrystalline $BaTiO_3$ by positron annihilation techniques

2009 J. Phys.: Condens. Matter 21 445902

(http://iopscience.iop.org/0953-8984/21/44/445902)

J. Phys.: Condens. Matter **21** (2009) 445902 (5pp) doi:10.1088/0953-8984/21/44/445902

Identifying defects in multiferroic nanocrystalline $BaTiO_3$ by positron annihilation techniques

R V K Mangalam[1], Mahuya Chakrabrati[2], D Sanyal[2], A Chakrabati[2] and A Sundaresan[1]

[1] Chemistry and Physics of Materials Unit, Department of Science and Technology Unit on Nanoscience, Jawaharlal Nehru Centre for Advanced Scientific Research, Jakkur PO, Bangalore 560064, India
[2] Variable Energy Cyclotron Centre, 1/AF Bidhannagar, Kolkata 700 064, India

E-mail: dirtha@veccal.ernet.in and sundaresan@jncasr.ac.in

Received 17 June 2009, in final form 4 September 2009
Published 15 October 2009
Online at stacks.iop.org/JPhysCM/21/445902

Abstract
Room temperature ferromagnetism in nanoparticles of otherwise nonmagnetic materials has been attributed to point defects at the surface of the nanoparticles. Here, we have employed positron annihilation spectroscopy to identify the nature of defects in multiferroic $BaTiO_3$ nanocrystalline materials with varying average particle sizes. Ratio curve analysis of the Doppler broadening profile to a reference profile suggests that the defect is an oxygen vacancy. The decrease of intensity of the intermediate lifetime component with increasing particle size indicates a decrease of surface defect concentration. The large defect concentration in nanocrystalline $BaTiO_3$ can explain the observed room temperature ferromagnetism.

(Some figures in this article are in colour only in the electronic version)

1. Introduction

Recently, there has been a great deal of interest in the study of magnetism in nonmagnetic semiconductors diluted with magnetic impurities due to possible applications in spin-based electronic systems [1]. However, there are controversies over the existence or absence of ferromagnetism in many of these materials [2]. Even if there is magnetism, the origin seems not to be intrinsic to the main phase and possibly associated with magnetic impurity phases [3–5]. Meanwhile, magnetism in thin films of several nonmagnetic oxides such as HfO_2, ZnO and TiO_2 without magnetic impurities has been reported, but the appearance of magnetism is very sensitive to preparation conditions. The origin of magnetism in these films has been suggested to be due to oxygen vacancies [6–8]. Theoretical studies have shown that neutral cation vacancies, for example Hf vacancies, should be responsible for magnetism in HfO_2 [9]. Very recently, nanoparticles of inorganic materials which include otherwise nonmagnetic oxides such as CeO_2, Al_2O_3, MgO, ZnO, In_2O_3 and SnO_2, nitrides, chalcogenides and other functional materials like superconductors and ferroelectrics were shown to be ferromagnetic at room temperature [10–14]. Conversely, the bulk samples obtained by sintering the nanoparticles at high temperatures became diamagnetic. The magnetism in these nanoparticles has been suggested to be intrinsic and originates from cation or anion vacancies at the surfaces of nanoparticles depending on the nature of cations. In fact, the surface ferromagnetism has been envisaged to be a universal feature of nanoparticles of inorganic materials [14]. Very recently, it has been demonstrated from both experiments and first-principles calculations that the classic ferroelectric material $BaTiO_3$ (BTO) becomes multiferroic when it is made at the nanoscale [15]. Multiferroics are materials having ferroelectric and ferromagnetic properties simultaneously and a coupling between these two order parameters makes these materials magnetoelectric [16]. In the case of nanocrystalline BTO, the ferroelectricity comes from the core while the ferromagnetism is confined to the surface of the nanocrystals. Oxygen vacancies at the surface of the nanocrystalline BTO are found to be responsible for ferromagnetism. Further, a strong coupling between a surface polar phonon and spin

was shown to result in a magnetocapacitance effect at room temperature [15].

As the source of ferromagnetism in these nanoparticles is believed to be due to surface defects, positron annihilation spectroscopy (PAS) has been employed to characterize these defects, since PAS can provide valuable information about the nature of defects as the annihilation parameters are sensitive to lattice imperfections. In PAS, the positron may be trapped in crystal defects, i.e. the wavefunction of the positron is localized at the defect site until annihilation and is thus useful to characterize the defects in the sample [17, 19]. PAS has been used to characterize defects in metals, semiconductors and polymers. Further, it has been shown that PAS is an excellent technique for studying open-volume defects, vacancy–impurity complexes and for identifying the sublattice occupied by the dopants. In this report, we have investigated the BTO nanoparticles of different sizes using PAS and correlate the results with the saturation magnetization.

2. Experimental section

BTO nanoparticles were prepared by the polymer precursor method using high purity (99.99%) $BaCO_3$ and titanium (IV) isopropoxide as starting materials [15, 20, 21]. A stoichiometric quantity of titanium (IV) isopropoxide was added to a mixture of ethanol and acetic acid (3:1 volume ratio) and stirred continuously. After 2 h, barium citrate solution, prepared with the required amount of citric acid and $BaCO_3$, was added. Polyvinyl alcohol solution was finally added to the mixture, followed by continuous stirring until the formation of a white sol. The sol was centrifuged and dried at room temperature. Thermogravimetric analysis of the as-prepared sample showed that the decomposition of organic components occurs around 500 °C. In order to completely remove the organic part, the sample was heated at 700 °C in oxygen. The 700 °C treated sample was further heated at 1000 °C for 1 h to slightly increase the particle size. Finally, to get a micron-sized BTO, the nanocrystalline BTO was sintered at 1200 °C for 12 h. Phase purity of the samples was analyzed by the x-ray diffraction method. Morphology and particle size were analyzed by field emission scanning electron microscopy (FESEM) using a NOVA NANOSEM 600 (FEI, The Netherlands). The magnetic measurements were carried out with a vibrating sample magnetometer in a physical property measurement system (Quantum Design, USA).

For positron annihilation studies a 10 μCi ^{22}Na source of positrons (enclosed between 2 μm thin nickel foils) has been sandwiched between two identical and plane faced pellets [22–24]. The positron annihilation lifetimes have been measured with a fast–slow coincidence assembly [22–24]. The detectors are 25 mm diameter × 25 mm long cylindrical BaF_2 scintillators optically coupled to Philips XP2020Q photomultiplier tubes. The resolving time (full width at half-maximum (FWHM)) measured with a ^{60}Co source and with the windows of the slow channels of the fast–slow coincidence assembly set to select pulses corresponding to 300–550 keV in one channel and 700–1320 keV in the other, is 250 ps. For each positron annihilation lifetime spectrum about 10^6 coincidence counts have been recorded. For each sample at least five to six positron annihilation lifetime spectra of about 10^6 coincidence counts have been recorded to ensure the repeatability of the measurements. Measured positron annihilation lifetime spectra have been analyzed by the computer program PATFIT-88 [25] with necessary source corrections (446 ps of 4% intensity) to evaluate the possible lifetime components τ_i and their corresponding intensities I_i. For the coincidence Doppler broadening of annihilation γ-radiation (CDBAR) measurement, two identical HPGe detectors (efficiency: 12%; type: PGC 1216sp of DSG, Germany) having an energy resolution of 1.1 keV at 514 keV of ^{85}Sr have been used as two 511 keV γ-ray detectors. The CDBAR spectrum has been recorded in a dual-ADC-based multiparameter data acquisition system (MPA-3, FAST ComTec, Germany). The peak-to-background ratio of this CDBAR measurement system, with $\pm\Delta E$ selection, is $\sim 10^5$:1 [26, 27]. CDBAR spectra have also been analyzed by constructing the ratio curve [27–30].

3. Results and discussion

XRD patterns confirmed that all the samples were single phase with a tetragonal structure. FESEM images of samples heated at 700, 1000 and 1200 °C are shown in figures 1(a)–(c). The 700 °C heat-treated sample shows rods containing assemblies of nanoparticles with an average diameter of 60 nm (figure 1(a)). Figure 1(b) shows the 100 nm nanoparticles prepared by 1000 °C heat treatment. The FESEM image of the bulk BTO sample (figure 1(c)), obtained by sintering the pressed nanoparticles at 1200 °C, shows the average grain size to be around 2 μm.

The magnetic measurements carried out on 60 nm, 100 nm and 2 μm (bulk) samples and are shown in figure 1(d). The first two samples clearly show ferromagnetism at room temperature whereas the 2 μm sample shows a diamagnetic curve as expected for the bulk BTO. The saturation magnetization of smaller (60 nm) particles is higher (0.002 98 emu g^{-1}) than that (0.002 13 emu g^{-1}) of bigger particles which is consistent with the suggestion that surface defects decrease with increasing particle size [14]. Since there are no magnetic elements involved in the preparation of BTO nanoparticles and there was no contamination of magnetic materials during characterization, the ferromagnetism is intrinsic to the nanoparticles. Further evidence for the magnetism comes from the magnetocapacitance effect observed in the nanocrystalline BTO [15].

Table 1 shows the value of the positron lifetimes and their corresponding intensities for all three BTO samples. Figure 2 shows the experimental positron lifetime spectrum, $N(t)$ versus t, and the free (three lifetime components) fitting curve by PATFIT-88 computer code for both 60 nm and bulk $BaTiO_3$ samples. The free fitting of all the positron lifetime spectra for all three samples (60 nm, 100 nm and 2 μm) are found to be best fitted (variance of fit is 1/channel) with three lifetime components fitting, yielding a very long (1400–2000 ps) lifetime component (τ_3) with an intensity (I_3) of 1–4%. This component is due to the formation of orthopositronium and its subsequent decay as parapositronium

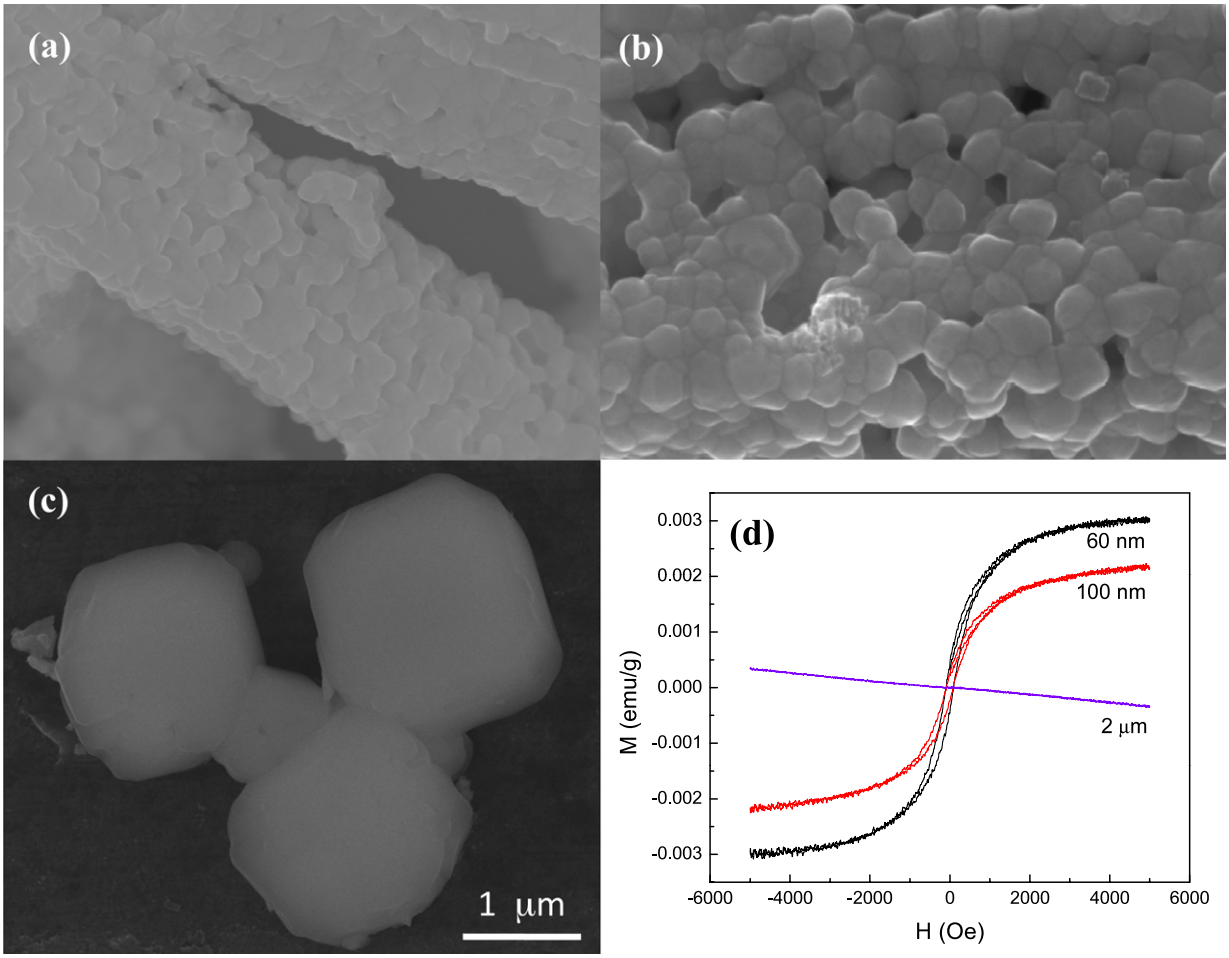

Figure 1. FESEM micrographs of $BaTiO_3$ nanoparticles treated at (a) 700 °C, (b) 1000 °C and (c) 1200 °C. (d) Room temperature magnetic hysteresis of 60 nm, 100 nm and 2 μm size $BaTiO_3$.

Table 1. Positron lifetimes and their corresponding intensities.

Sample	τ_1 (ps)	τ_2 (ps)	I_2 (%)	τ_3 (ps)	I_3 (%)
60 nm	163 ± 2	348 ± 10	51 ± 1	1965 ± 100	4 ± 0.2
100 nm	165 ± 2	322 ± 08	48 ± 1	1631 ± 100	2 ± 0.2
2 μm	161 ± 2	353 ± 10	18 ± 1	1465 ± 100	1 ± 0.2

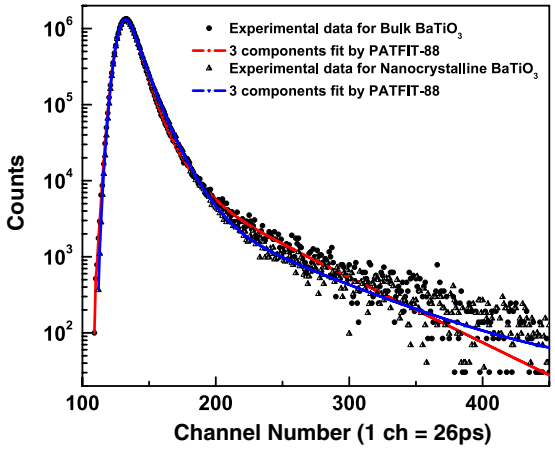

Figure 2. The experimental positron lifetime spectrum, $N(t)$ versus t, and the three lifetime components fitting curve by PATFIT-88 computer code for both 60 nm and bulk $BaTiO_3$.

by pick-off annihilation processes [22, 23]. In polycrystalline samples, there always exist microvoids where positronium formation is favorable. The short lifetime component (τ_1) of 163 ± 2 ps is generally attributed to the free annihilation of positrons. The presently observed τ_1 of 163 is very close to the lifetime value of 166 ± 1 ps observed by Macchi *et al* [31] for well-annealed $BaTiO_3$ single crystal. Suvegh *et al* [18] has reported τ_1 of 160 ± 4 ps for fine powdered $BaTiO_3$, which is also very close to the presently observed value. The theoretically calculated free positron lifetime in bulk $BaTiO_3$ is 152 ps, which is slightly less than the presently observed value, 163 ± 2 ps [17]. The intermediate lifetime component, τ_2, arises from the annihilation of positrons at defect sites. The presently observed value of τ_2 is 348 ± 10 ps, which is believed to come from the annihilation of positrons at vacancy complexes formed between the oxygen vacancies and the metal ion vacancies. It is obvious from table 1 that I_2 (the intensity of the intermediate lifetime component) is higher in 60 and 100 nm particles than in the bulk sample and decreases with increasing particle size. The intensity (I_2) of the

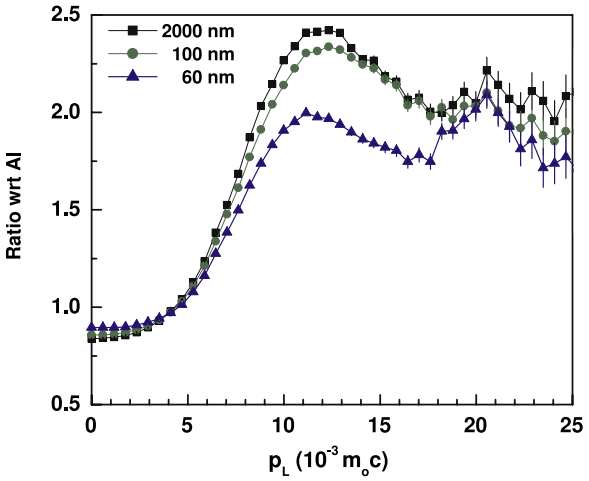

Figure 3. Area normalized ratio curve of 60 nm, 100 nm and 2 μm size $BaTiO_3$ CDBAR spectra with respect to defect-free 99.9999% purity Al CDBAR spectrum.

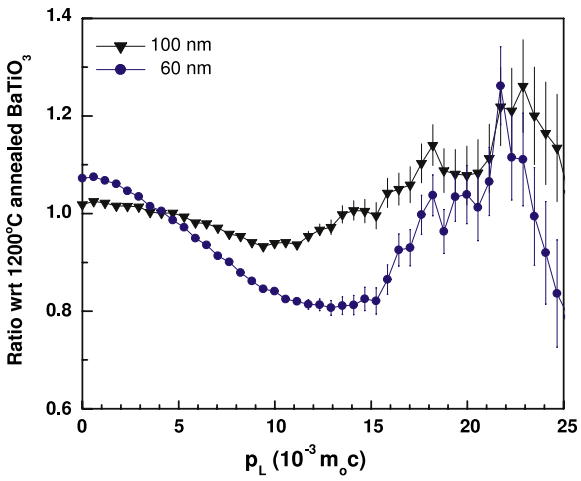

Figure 4. Area normalized ratio curve of 60 nm and 100 nm size $BaTiO_3$ CDBAR spectra with respect to 2 μm size $BaTiO_3$ CDBAR spectrum.

intermediate lifetime component decreases from 48% to 18% due to the increase of particle size from 60 nm to 2 μm. This indicates that, as the grain size decreases, positrons diffuse (typical diffusion length of positrons in a material ~200–300 nm) towards the grain surfaces and are trapped in these defect sites present in the grain surfaces. Thus, as the particle size increases, the decrease of magnetization or the suppression of magnetism is in agreement with the decrease of surface defect concentration.

In order to identify the nature of defects in BTO samples, the ratio curve analysis technique of the CDBAR spectra has been used [17, 27–30]. Figure 3 shows the area normalized ratio curve of CDBAR spectra of the three samples (60 nm, 100 nm and 2 μm) with respect to the CDBAR spectrum of the defect-free 99.9999% purity Al sample. All the ratio curves (figure 3) show one major peak at $\sim 11 \times 10^{-3}\ m_0c$ and another peak at $\sim 20 \times 10^{-3}\ m_0c$. Using the relation, $E_{k.E}(\text{eV}) = p_{L^2}/4m_0$, the kinetic energy of electrons corresponding to the momentum $p_L = 20 \times 10^{-3}\ m_0c$ comes out to be ~51 eV. In general, the peak at momentum value $\sim 11 \times 10^{-3}\ m_0c$ in the ratio curve with respect to Al mainly comes from the annihilation of positrons with the 2p electrons of oxygen [27, 29, 32] and some contributions coming from the annihilations with the 3d electrons of Ti and 5p electrons of Ba, while the peak at momentum value $\sim 20 \times 10^{-3}\ m_0c$ comes from the annihilation of positrons with the core electrons of Ti. From figure 3 it is clear that the peak height at $\sim 11 \times 10^{-3}\ m_0c$ decreases with decreasing particle size, while the peak height at $\sim 20 \times 10^{-3}\ m_0c$ is almost the same for all three samples, which indicates the presence of a significant amount of oxygen vacancies in the 60 nm particles than in the bulk sample. This is also clear from figure 4 where the area normalized ratio curves of 60 and 100 nm samples have been plotted with respect to the bulk BTO CDBAR spectrum. Figure 4 also shows a broad dip in the momentum value $\sim 11 \times 10^{-3}\ m_0c$. This indicates lesser annihilation of positrons with the 2p electrons of oxygen in the 100 and 60 nm samples compared to the bulk sample. Thus, from ratio curve analysis, defects in the 100 and 60 nm samples have been identified as oxygen vacancies. Each oxygen vacancy is expected to donate two electrons to the empty d state of a single Ti^{4+} ion to produce a Ti^{2+} ion or one electron each to two Ti^{4+} ions, probably situated on either side of the oxygen vacancy, to make them Ti^{3+} ions [15, 33]. Both configurations result in the ferromagnetic ground state due to Hund's rule coupling provided there is a minimum concentration of oxygen vacancies required for magnetic percolation. The fact is that a relatively large value of I_2 and the observed ferromagnetism in 60 nm and 100 nm samples indicate the presence of a critical concentration of oxygen vacancies on the surface of the particles. In the case of the bulk sample, the low value of defects is consistent with the observed diamagnetism.

4. Conclusions

Nanocrystalline $BaTiO_3$ with an average size of 60 and 100 nm show ferromagnetic hysteresis at room temperature whereas the 2 μm sample exhibits diamagnetism as expected for a bulk sample. Positron annihilation studies show lesser annihilation of positrons with the 2p electrons of oxygen in the 100 and 60 nm samples compared to the bulk sample, indicating the presence of oxygen vacancies. Thus, the observed ferromagnetism in nanocrystalline $BaTiO_3$ samples can be correlated with the presence of oxygen vacancies at the surface of the particles.

Acknowledgment

One of the authors (MC) gratefully acknowledges the CSIR, Government of India for providing financial assistance.

References

[1] Dietl T, Ohno H, Matsukura F, Cibert J and Ferrand D 2000 *Science* **287** 1019
[2] Seshadri R 2005 *Curr. Opin. Solid State Mater. Sci.* **9** 1

[3] Zajac M, Doradzinski R, Gosk J, Szczytko J, Lefeld-Sosnowska M, Kaminska M, Twardowski A, Palczewska M, Grzanka E and Gebicki W 2001 *Appl. Phys. Lett.* **78** 1276
[4] Bonanni A, Kiecana M, Simbrunner C, Li T, Sawicki M, Wegscheider M, Quast M, Przybylinska H, Navarro-Quezada A, Jakiela R, Wolos A, Jantsch W and Dietl T 2007 *Phys. Rev.* B **75** 1252
[5] Abraham D W, Frank M M and Guha S 2005 *Appl. Phys. Lett.* **87** 252502
[6] Venkatesan M, Fitzgerald C B and Coey J M D 2004 *Nature* **430** 630
[7] Hong N H, Sakai J, Poirot N and Brize V 2006 *Phys. Rev.* B **73** 132404
[8] Hong N H, Sakai J and Brize V 2007 *J. Phys.: Condens. Matter* **19** 036219
[9] Pemmaraju C D and Sanvito S 2005 *Phys. Rev. Lett.* **94** 217205
[10] Sundaresan A, Bhargavi R, Rangarajan N, Siddesh U and Rao C N R 2006 *Phys. Rev.* B **74** 161306
[11] Hu J, Zhang Z, Zhao M, Qin H and Jiang M 2008 *Appl. Phys. Lett.* **93** 192503
[12] Shipra, Gomathi A, Sundaresan A and Rao C N R 2007 *Solid State Commun.* **142** 685
[13] Madhu C, Sundaresan A and Rao C N R 2008 *Phys. Rev.* B **77** 201306
[14] Sundaresan A and Rao C N R 2009 *Nano Today* **4** 96
[15] Mangalam R V K, Ray N, Waghmare U V, Sundaresan A and Rao C N R 2008 *Solid State Commun.* **149** 1
[16] Schmid H 1994 *Ferroelectrics* **162** 317
[17] Ghosh V J, Nielsen B and Friessnegg T 2000 *Phys. Rev.* B **61** 207
[18] Suvegh K, Domjan A, Tarsoly R and Vertes A 1996 *J. Radioanal. Nucl. Chem.* **211** 255
[19] Sanyal D, Roy T K, Chakrabarti M, Dechoudhury S, Bhowmick D and Chakrabarti A 2008 *J. Phys.: Condens. Matter* **20** 045217
[20] Cho W S 1998 *J. Phys. Chem. Solids* **59** 659
[21] Jana A, Kundu T K, Pradhan S K and Chakravorty D 2005 *J. Appl. Phys.* **97** 044311
[22] Hautojarvi P and Corbel C 1995 *Positron Spectroscopy of Solids* ed A Dupasquier and A P Mills Jr (Ohmsha, Amsterdam: IOS Press)
[23] Krause-Rehberg R and Leipner H S 1999 *Positron Annihilation in Semiconductors* (Berlin: Springer)
[24] Sanyal D, Banerjee D and De U 1998 *Phys. Rev.* B **58** 15226
[25] Kirkegaard P, Pedersen N J and Eldroup M 1989 *Report of Riso National Lab (Riso-M2740)*
[26] Lynn K G and Goland A N 1976 *Solid State Commun.* **18** 1549
[27] Sanyal D, Chakrabarti M, Roy T K and Chakrabarti A 2007 *Phys. Lett.* A **371** 482
[28] Chakrabarti M, Sarkar A, Sanyal D, Karwasz G P and Zecca A 2004 *Phys. Lett.* A **321** 376
[29] Dutta S, Chakrabarti M, Chattopadhyay S, Jana D, Sanyal D and Sarkar A 2005 *J. Appl. Phys.* **98** 053513
[30] Dutta S, Chattopadhyay S, Sarkar A, Chakrabarti M, Sanyal D and Jana D 2009 *Prog. Mater Sci.* **54** 89
[31] Macchi C, Somoza A, Dupasquier A, Lopez Garcia A and Castro M 2001 *J. Phys.: Condens. Matter* **13** 5717
[32] Myler U and Simpson P J 1997 *Phys. Rev.* B **56** 14303
[33] Stoneham A M, Gavartin J, Shluger A L, Kimmel A V, Muoz Ramo D, Rnnow H M, Aeppli G and Renner C 2007 *J. Phys.: Condens. Matter* **19** 255208